

Glycerol sorbent selection and optimized conditions for ethyl biodiesel purification by response surface methodology

Flavia D. Santos¹, Leyvison Rafael V. da Conceição², Domingos S. Giordani³,
Heizir F. de Castro^{4*}

Department of Chemical Engineering, Engineering School of Lorena, University of São Paulo
Estrada Municipal do Campinho s/n, 12602-810, Lorena, São Paulo – Brazil
*e-mail: heizir@dequi.eel.usp.br

Abstract— *The feasibility of using alternative and commercial sorbents for dry washing biodiesel was quantitatively examined. Rice husk ash (RHA) and Amberlite showed similar performance and their applications in adsorbing glycerol were determined by response surface methodology. A 2² face centered composite design was employed to analyze the combined effect of sorbent concentration and temperature on glycerol removal. The statistical analysis indicated that levels of 2.1% (RHA) and 3.7% (Amberlite) at 30 °C maximized the glycerol removal with minimum loss of adsorbate. Under optimal conditions, the sorbents were used for purifying ethyl biodiesel samples from palm kernel oil. Both sorbents were quite efficient in removing glycerol, providing samples containing glycerol values lower than 0.01% that meet the required standard to be used as a fuel. The high quality of the purified samples was also demonstrated by the ethyl esters contents (> 98.0%), viscosity (< 4.0 mm² s⁻¹) and density (\cong 867 kg m⁻³) values. Rice husk ash was also able to remove monoacylglycerols and diacylglycerols, thus its structure, composition and adsorption kinetics were further assessed to better understand its property as sorbent*

Keywords— *Biodiesel, dry washing, glycerol, sorbent, factorial design.*

I. INTRODUCTION

The transesterification of feedstocks based on triacylglycerols with monohydric alcohols yields crude biodiesel containing mono-alkyl ester as main product and glycerol as byproduct. Crude biodiesel must be submitted by a purification step to remove various impurities (glycerol, unconverted triacylglycerols, monoacylglycerols, diacylglycerols, free fatty acids, water, catalyst, soaps, among others) to prevent a significant damage to diesel engines [1,2]. Therefore, this purification process becomes very important to meet the ASTM D 6751 (USA) (American Society for Testing and Materials) and EN 14214 (European standard), quality standards for commercial biodiesel production [3].

The purification of biodiesel can be carried out by wet and/or dry washing. Until recently, water washing was the most common purification method. Nowadays, both methods are generally accepted and applied on a commercial scale [1,4,5]. Dry washing removes contaminants from crude biodiesel by adsorption, or by passing crude biodiesel through a packed bed running under specific flow rates. Different commercial adsorbent materials were developed specifically for treating crude biodiesel, such as Magnesol[®] (magnesium silicate) and ion exchange resins (Purolite PD206[®], Amberlite Dry BD10 and Lewatit GF 202). In addition, alternative and low-cost sorbents (bentonite, starch derivatives, silica, among others) have already been investigated to reduce the overall cost of this procedure [6,7,8].

Berrios et al. [9] studied the purification of methyl biodiesel from fried oil using bentonite clay as sorbent in comparison with the performance attained by commercial resins, Magnesol and Lewatit. The results showed that, among all tested sorbents, bentonite could effectively remove soap, methanol and glycerol. The feasibility of using natural adsorbents such as cellulose and starch obtained from different sources (maize, potato, cassava and rice), for biodiesel purification was investigated by Gomes et al. [10]. All natural adsorbents studied showed good efficiency in removing impurities from biodiesel when compared to the aqueous washing technique and adsorption with a commercial resin, Select 450.

Vasques et al. [11] assessed various adsorbents such as zeolite, activated alumina, and activated coals from babassu coconut in their natural form or modified with HNO₃. The results obtained showed that the activated coal modified with HNO₃ was the most effective in removing intermediates, i.e. the glycerol, monoacylglycerols and diacylglycerols that are present in the biodiesel produced from soybean oil.

The purification of methyl biodiesel from palm oil using Magnesol and diatomaceous earth was performed by Na-Ranong et al. [12]. The authors observed that it is possible to reduce up to 80% of glycerol concentration using 1% (wt) of Magnesol

and 3% (wt) of diatomaceous earth in 10 min at a temperature range from 65 to 80 °C. De Paula et al. [13] compared the effectiveness of purification methods of biodiesel from residual fried oil by aqueous washing and adsorption with bauxite, bentonite clay and attapulgite. All adsorbents were able to remove soap, especially bentonite and bauxite stands out in removing free glycerol.

In short, there have been many studies for the purification of methyl biodiesel using adsorption techniques; however, the application of alternative adsorbents for the purification of ethyl biodiesel is still scarce. In view of the difficulties reported to separate glycerol and the ethyl ester phases, dry washing approach is a promising alternative [14,15]. Thus, the objective of this work was to evaluate the performance of different adsorption agents on the purification of ethyl biodiesel from palm kernel oil taking the efficiency demonstrated by a conventional purification method (aqueous washing) as control parameter. For the selected adsorbents, the combined effect of adsorbent concentration and temperature on glycerol removal was studied using the response surface methodology.

II. MATERIAL AND METHODS

2.1 Chemicals

Clay Cloisite 15-A (Southern Clay), silica powder (Grace Davison), rice husk ash (RHA) (Cotrisel/Parana), Amberlite BD10 DRY (Rohm & Haas Chemicals Ltd) and Purolite PD206 (Purolite Corporation) were tested as sorbents. All sorbents were activated with methanol prior to their use following recommendation for commercial resins [16]. Niobium oxide impregnated with sodium hydroxide solution ($\text{Nb}_2\text{O}_5/\text{Na}$) obtaining according to the methodology previously described was used as a catalyst (Carvalho, 2011). Ethanol (99% Vetec) was used as acylant and refined and bleached palm kernel oil was kindly supplied by Agropalma (Para, Brazil). Other reagents used were: glycerol (99.7%, Cromoline), methanol (99%, Vetec), tert-butanol (Cromoline), (hexane (Cromoline), acetic acid (99.7%, Cromoline), ammonium acetate (Synth), acetylacetone (Vetec), sodium metaperiodate (Synth), anhydrous sodium sulfate (99%, Cromoline) and sodium hydroxide (Vetec).

2.2 Sorbent screening tests

The screening of sorbents was carried out by means of adsorption tests using 10 mL of alcoholic glycerol (5%) solution and different adsorbents (5% w/v), followed by incubation in a ultrasonic batch cleaner (model USC 1800-UltraSonic Cleaner-Unique) at 30 °C for 2 h. Then, mixtures were centrifuged (centrifugal Model 206-BL, Excelsa II-Fanem) at 1570 x g during 30 min. The supernatant was weighed to determine the mass recovered (Eq. 1) and then the residual level of glycerol quantified (methodology described in 2.6) was used to calculate the percentage of glycerol removal (Eq. 2).

$$\% Wr = \frac{S_{rw}}{S_{iw}} \times 100 \quad (1)$$

$$\% Gr = \frac{G_{wi} - G_{wf}}{G_{wi}} \times 100 \quad (2)$$

In which: Wr is the mass of the tested solution recovered; S_{rw} is the recovered mass of solution, S_{iw} is the initial mass of the solution; Gr is the glycerol removal, G_{wi} is the initial glycerol mass and G_{wf} is the final glycerol mass.

2.3 Experimental design and optimization by RSM

A 2^2 face centered central composition design (CCD) with three coded levels leading to eleven sets of experiments was performed. The range and the levels of the independent variables were: X_1 absorbent mass (2-8%) and X_2 temperature (30-50 °C). The glycerol removal (Y_1) and mass recovered (Y_2) were taken as the dependent variables or responses of the design experiments. The "Design expert" (version 9.0) and "Statistica" (version 12.5) softwares were used for regression and graphical analyses of the data obtained.

2.4 Preparation of raw biodiesel samples

Biodiesel synthesis was performed in 500 mL reactor coupled with a reflux condenser containing 40 g of palm kernel oil and 150 g of anhydrous ethanol. Niobium oxide impregnated with sodium ($\text{Nb}_2\text{O}_5/\text{Na}$) previously activated in an oven (200 °C for 24 h) was used as catalyst at proportion of 10% in relation to the oil mass. The experiments were carried out at 78.5 °C under mechanical agitation 600 rpm for 5 h [17]. At the end of the reaction, the mixture was subjected to natural cooling for approximately one hour and separation of the catalyst was carried out through by vacuum filtration. The glycerol quantification in the crude biodiesel was found to be $0.29 \pm 0.03\%$.

2.5 Purification Processes

2.5.1 Wet Washing

A sample of 100 mL of crude biodiesel was transferred to a 500 mL separatory funnel, to which 100 mL of distilled water at 30 °C was added. Vigorous agitation was then carried out and the mixture was allowed to stand for 30 min for phase separation. This procedure was performed three times to remove the free glycerol formed as a by-product. Residual ethanol was evaporated using a rotary evaporator at 80 °C for 50 min. Residual water was removed by the addition of anhydrous sodium sulfate. The purification was carried out in duplicate [17].

2.5.2 Dry washing

Samples of 30 mL of crude biodiesel and the selected absorbents at conditions, concentration (% w/v) and temperature, predicted by the numerical optimization method were transferred to a 50 mL Falcon tubes and placed in an ultrasound bath for 2 h. Then, the mixtures were centrifuged (1570 x g for 15 min) and residual ethanol removed in a rotary evaporator at 80 °C for 50 min. The purification was performed in duplicate.

2.6 Characterization of purified biodiesel

The determination of free glycerol contents was carried out by the methodology developed by Bondioli and Bella [18]. The method is based on the oxidation of free glycerol with periodic acid, resulting in formaldehyde which reacts with acetyl acetone in the presence of ammonium acetate, leading to the formation of 3,5-diacetyl-1,4-dihydrolutidine. The spectrophotometric analyses were carried out at 410 nm using a UV-visible spectrophotometer (Varian, Model Cary 50 Conc). The concentration of free glycerol was calculated based on the equation obtained from the calibration curve $Abs_{410\text{ nm}}$ versus glycerol concentration (correlation coefficient, $R^2 = 0.9986$).

Purified ethyl esters dissolved in deuterated chloroform were analyzed with a ^1H NMR (Mercury-300 MHz, Varian) spectrometer using 0.3% TMS as the internal standard. The conversion of triacylglycerol (TG) to their ethyl esters was determined by the methodology and equation validated by Paiva et al. [19]. Residual acylglycerol and ethyl esters were analyzed at 40 °C using an Agilent 1200 series liquid chromatograph (Agilent Technologies, USA) equipped with an evaporative light scattering detector and Gemini C-18 (5 μm , 150 \times 4.6 mm, 110 Å) column following methodology described by Andrade et al. [20].

The ethyl ester viscosity was determined according to the standard method ASTM D 445 with a LVDVII Brookfield viscosimeter (Brookfield Viscometers Ltd, England) equipped with a CP 42 cone at 40 °C using 0.5 mL of sample. Density value was determined according to the standard method ASTM D 4052 with a DMA 35N EX digital densimeter (Anton Paar) at 20 °C using 2 mL of sample.

2.7 Characterization of the selected sorbent

The morphology of the RHA was analyzed by scanning electron microscopy (SEM) in a LEO 145VP equipment with EDS and magnification of 1000 and 2000X. The chemical composition of the selected sorbent was determined by X-Ray Fluorescence Spectrometry (XRF) using an Axios MAX model, PANalytical spectrometer. The crystallinity was determined by X-ray diffraction (XRD) in a PANalytical diffractometer (Empyrean model) using CuK ($= 1.5418 \text{ \AA}$) as incident radiation, operating at 40 kV and 30 mA. The identification of the sorbent morphological structure was observed by X-ray diffraction; using CuK radiation source, with 2° angle varying from 8 to 70° .

The specific surface area and the pore size were measured by adsorption-desorption isotherms (N_2) at 77 K using BET (Brunauer, Emmett and Teller) method in Quantachrome equipment (new 1000 model). The infrared spectra were recorded on a spectrum GX FT-IR system Perkin Elmer spectrometer. Samples were pelletized with KBr, and spectra were obtained from the accumulation of a total of 32 scans in the range of 4000 to 400 cm^{-1} with resolution of 4 cm^{-1} .

III. RESULTS AND DISCUSSION

3.1 Screening tests for sorbent selection

The ability of five different sorbents in removing glycerol from synthetic medium was assessed for further application in the ethyl biodiesel purification. Table 1 shows the values generated by the action of each sorbent in terms of glycerol removal and mass recovered. Their pH values were also displayed with the purpose of establishing a correlation of this factor with

their performance in the adsorptive process. Two commercial sorbents (polymeric resins) developed specifically for biodiesel purification were also assessed in order to select the most efficient as reference to the tested alternative adsorbents.

TABLE 1
GLYCEROL REMOVAL AND MASS RECOVERED USING DIFFERENT SORBENTS, AND CORRELATION WITH THEIR RESPECTIVE pH VALUES

Adsorbents	pH	Glycerol removal (%)	Mass recovered (%)
Clay Cloisite 15-A	7.8	46.5 ± 1.2	94.0
Silica powder	3.4	61.0 ± 1.1	92.5
Rice husk ash	9.2	81.5 ± 1.1	91.5
Amberlite BD10DRY	2.8	83.0 ± 1.1	93.5
Purolite PD206	2.7	79.0 ± 1.4	92.0

Among the tested commercial resins, Amberlite BD10DRY showed a better performance than Purolite PD206, leading to a glycerol reduction of $83.1 \pm 1.1\%$. Concerning the alternative adsorbents, the lowest glycerol removal was found for silica powder and clay Cloisite A-15 (organophilic Montmorillonite), resulting in a reduction of $60.8 \pm 1.1\%$ and $46.7 \pm 1.2\%$, respectively. On the other hand, the highest adsorption degree was found for RHA, allowing a glycerol removal percentage of $81.7 \pm 1.1\%$. Thus, RHA and Amberlite were selected as adsorption agents for further investigations.

With respect to the adsorbents pH values, no correlation was verified with glycerol removal, since both RHA and Amberlite BD10DRY achieved a similar percentage of glycerol reduction, despite their different pH values, 9.2 and 2.8 respectively. Moreover, Amberlite BD10DRY, Purolite PD206 and silica powder have similar pH values, but the difference in their performance is notable.

3.2 Statistical analysis

The optimal conditions that simultaneously maximize glycerol removal and mass recovered for the selected sorbents were determined by a factorial design. The experimental matrix together with the data for each response factor is shown in Table 2. The influence of the studied variables on the responses was different for both evaluated sorbents. For Amberlite, the glycerol reduction varied from 64.6 to 80.0% and the highest glycerol removal was obtained when the independent factors were taken at their lowest levels (run 1). Under such conditions, the mass recovered from the trial sample (5% glycerol in ethanol) was minimized (94% mass recovered). For RHA, the glycerol reduction varied from 70.4 to 86.2% and the highest glycerol removal was attained at the highest sorbent concentration and the lowest temperature (run 3), at the expense of increasing glycerol loss (mass recovered was only 65.2%).

TABLE 2
EXPERIMENTAL DESIGN AND RESULTS ACCORDING TO THE FACE-CENTRED COMPOSITE DESIGN

Run	Variables		Amberlite BD10DRY		Rice husk ash	
	X ₁ Adsorbent mass (%)	X ₂ Temperature (°C)	Glycerol removal (%)	Mass recovered (%)	Glycerol removal (%)	Mass recovered (%)
1	2(-1)	30(-1)	80.00	94.95	75.75	94.00
2	2(-1)	50(+1)	69.40	94.40	70.40	89.75
3	8(+1)	30(-1)	73.50	91.60	86.10	65.20
4	8(+1)	50(+1)	64.65	88.20	83.80	52.20
5	8(+1)	40(0)	72.00	90.50	83.20	63.10
6	2(-1)	40(0)	77.10	95.60	73.65	93.50
7	5(0)	50(+1)	70.15	90.00	75.50	71.60
8	5(0)	30(-1)	76.75	93.00	77.90	90.00
9	5(0)	40(0)	77.55	92.00	73.30	80.00
10	5(0)	40(0)	75.00	91.80	71.65	80.70
11	5(0)	40(0)	74.60	92.60	74.00	81.80

Results displayed in Table 2 were used to estimate the main variable effects and their interactions. The most important factor was the sorbent concentration, since it presented a significant effect (95% confidence level) for both response variables. For the mass recovered response variable (Y_2), the statistical analysis showed that the significant factors for both adsorbents were the linear variable (X_1) sorbent concentration and (X_2) temperature ($p < 0.05$), and their effects were negative. In contrast, the influence of the factors on the glycerol removal (Y_1) was different for each evaluated sorbent. For Amberlite, the statistical analysis showed significant linear and quadratic effects for both studied variables at 95% confidence level. On the other hand, for RHA, the glycerol removal showed linear and quadratic effects for the sorbent concentration (X_1) besides a significant and negative linear effect for the temperature (X_2) at 95% confidence level. Based on the independent variables effects, a regression analysis was carried out to obtain mathematical models that represent the behavior of the experimental results. The models were composed of coefficients correspondent to significant effects (p -values < 0.05) and non-significant effects (p -values > 0.05), necessary to maintain hierarchy of the models [21]. The resulting models are shown in Table 3.

TABLE 3

MODEL EQUATIONS FOR THE RESPONSE SURFACES FITTED TO THE EXPERIMENTAL DATA CONSIDERING GLYCEROL REMOVAL (Y_1) AND MASS RECOVERED (Y_2) AS A FUNCTION OF THE SORBENT CONCENTRATION (X_1) AND TEMPERATURE (X_2).

Adsorbent	Model equation	R^2
Amberlite BD10DRY	$Y_1 = 92.05 - 2.75X_1 - 1.50X_2 + 1.10X_1^2 - 0.45X_2^2 - 0.20X_1X_2$	0.9370
	$Y_2 = 75.80 - 2.75X_1 - 4.35X_2 - 1.35X_1^2 - 2.45X_2^2 + 0.50X_1X_2$	0.9909
Rice husk ash	$Y_1 = 81.50 - 16.10X_1 - 5.95X_2 - 4.10X_1^2 - 1.60X_2^2 - 2.20X_1X_2$	0.9583
	$Y_2 = 73.70 + 5.55X_1 - 1.65X_2 + 3.80X_1^2 + 2.05X_2^2 + 0.75X_1X_2$	0.9780

The statistical analysis of these models indicated that they were statistically significant at 95% confidence level. In addition, the models did not show lack of fit ($p > 0.05$) and presented a high determination coefficients (R^2 between 0.94 and 0.99) explaining more than 94% of the variability in the responses. Thus, the equations were considered adequate for describing the glycerol removal as a function of the studied variables, and were used to plot the response surfaces as showed in Figs 1(a-d).

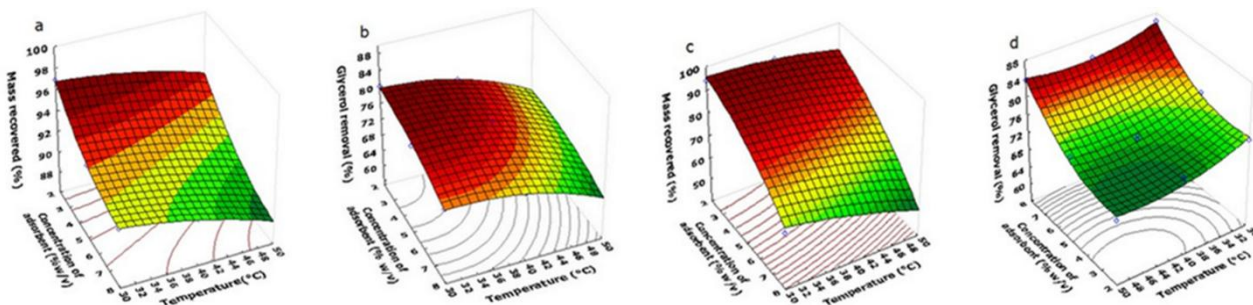


FIGURE 1. RESPONSE SURFACES DESCRIBED BY THE MODELS THAT REPRESENT THE MASS RECOVERED BY AMBERLITE BD10DRY (A) AND RICE HUSK ASH (C) AND GLYCEROL REMOVAL BY AMBERLITE BD10DRY (B) AND RICE HUSK ASH (D).

For Amberlite (Fig. 1a), to attain mass recovered higher than 90%, it is necessary to use this sorbent in the range of 2-8% at a temperature range of 30-45 °C. Different parameters were found for RHA and its concentration should be lower than 2.5% at a temperature range from 30 to 35 °C. On the other hand, to attain glycerol removal greater than 79% using Amberlite, the optimal sorbent concentrations were in the range of 2-5% (% w/v) at temperatures of 30-45 °C. For RHA, the model indicated that the sorbent concentration should be in the range of 6-8 (% w/v). However, the temperature has not significantly affected on the glycerol removal enabling to attain high adsorption percentage ($> 79\%$) throughout the studied temperature range (30 to 50 °C). Based on the two obtained models, a graphical optimization was conducted using the “Design-expert” software to attain optimum conditions for each adsorbent that maximize both response variables. A graphical optimization aims at obtaining values of independent variables that provide high glycerol removal and minimum loss of adsorbate. Table 4 shows the optimum conditions of sorbent concentration and temperature, as well as the prediction of mass recovered and glycerol removal obtained for each sorbent.

To confirm these results, adsorption assays were carried out using optimized conditions. Under these conditions, the differences between experimental and theoretical values were (6.5 and 3.7%) for the RHA and (1.6 and 1.1%) for the Amberlite BD10DRY relative to both response variables mass recovered and glycerol removal, respectively. These results showed that the models were well adjusted to the experimental data, and thus the study region was adequately described.

TABLE 4
OPTIMUM CONDITIONS FOR MASS RECOVERED AND GLYCEROL REMOVAL USING AMBERLITE BD10DRY AND RICE HUSK ASH AS SORBENTS

Condition	Amberlite BD10DRY	Rice husk ash
Optimum concentration (%)	3.7	2.1
Optimum temperature (°C)	30	30
Predicted mass recovered (%)	94.5	95.5
Experimental mass recovered (%)	96.0 ± 0.6	92.0 ± 1.12
Predicted glycerol removal (%)	80.0	76.0
Experimental glycerol removal (%)	79.0 ± 0.9	81.5 ± 1.3

3.3 Purification of ethyl biodiesel

The purification of crude biodiesel from palm kernel oil having average glycerol contents of $0.29 \pm 0.03\%$ was carried out by wet and dry washing methods. The applications of Amberlite BD10DRY and RHA were performed under optimum conditions, as determined by the experimental design (Table 4) taken the following parameters glycerol, ethyl esters, monoacylglycerols (MG) and diacylglycerols (DG) contents, density and viscosity values into consideration. As displayed in Table 5 all purification methods exhibited the ability to remove higher than 98% glycerol from the crude biodiesel providing samples containing glycerol values lower than 0.01% that meet the specification established by EN 14214 standard (0.02%). The high quality of the purified samples was also demonstrated by the ethyl esters contents ($> 98.0\%$), viscosity ($< 4.0 \text{ mm}^2 \text{ s}^{-1}$) and density ($\cong 867 \text{ kg m}^{-3}$) values.

TABLE 5
ANALYSIS OF THE BIODIESEL SAMPLES ACCORDING TO THE PURIFICATION METHOD

Property	Water washing	Dry washing		EN14214
		Amberlite BD10DRY	Rice husk ash	
Viscosity ($\text{mm}^2 \text{ s}^{-1}$)	3.55 ± 0.01	3.70 ± 0.12	3.75 ± 0.03	3.0-6.0
Density (kg m^{-3})	866.0 ± 0.6	868.5 ± 0.3	867.5 ± 0.3	850-900
Free glycerol (%)	0.001	0.01	0.004	0.02
Monoacylglycerol (%)	0.43 ± 0.01	0.77 ± 0.18	0.34 ± 0.01	0.70
Diacylglycerol (%)	0.05 ± 0.03	0.04 ± 0.03	0.05 ± 0.03	0.20
Triacylglycerol (%)	0	0	0	0.20
*Ethyl esters (%)	98.5 ± 1.4	98.4 ± 1.2	98.3 ± 1.7	96.50

Average values between HPLC and ¹HNMR analyses

Data quantified by ¹H NMR were consistent with those achieved by HPLC as displayed in Table 5, indicating that the purified biodiesel samples by both aqueous washing and adsorption with RHA attained residual glycerides at levels required, which are 0.70% and 0.20% for MG and DG, respectively. Furthermore, the purification of the crude biodiesel sample by RHA revealed the lowest MG contents (0.34%), which corresponds to a level of 50% lower than the limit to be within the EN 14214 specification. On the other hand, under the conditions established the sample purified with ion exchange resin Amberlite BD10DRY exhibited MG content above the acceptable limit.

Based on these results it can be concluded that both adsorbents were effective and allowed obtaining biodiesel samples having similar quality in relation to that one attaining by the conventional wet washing procedure. Comparatively, the wet washing method exhibits some disadvantages such as loss of product, requires large amount of water (each 100 L of biodiesel generates approximately 20 L of wastewater) and high cost, which corresponds to 60-80% of the total processing cost. In addition, the wastewater generated should be treated before its final discharge thus increasing operating costs [5,8].

In this way, the dry washing method using RHA to purify crude biodiesel can be a promising strategy since it is a low cost agricultural waste and provided better fuel quality without wastewater generation.

3.4 Rice husk ash characterization

Parameters such as specific surface area and pore diameter were used to describe the texture properties of RHA. The pore diameter of solid materials can be classified as microporous when their diameter is up to 20 Å, mesoporous in the range of 20 to 500 Å and macroporous when greater than 500 Å [22]. RHA presented pore volume and average pore diameter of 0.022 m³g⁻¹ and 36.5 Å, respectively. Therefore, the structures are purely mesoporous and possible limitations by glycerol diffusions are unlike to occur. The specific surface area was 12.0 m² g⁻¹, which is within the range (4.0–21.3 m² g⁻¹) reported for different samples of RHA [23].

The SEM observation of the RHA surface morphology as shows in Fig. 2 a,b allows confirming a “corn cob” format basically in two distinct structures, as already previously reported [24]. One of the regions is characterized by being denser and shows the effect of burning the outer epidermis, the region with the highest percentage of silica [25,26]. It is also possible to note the presence of a porous region, which is supposed to be formed by the loss of the less dense organic compounds during combustion [24]. The presence of this macroporous structure gives the ashes larger contact surface, making easy the diffusion of the species to be adsorbed.

The mineralogical characterization of RHA by XRD (Fig. 3) demonstrated the presence of crystalline silica in the form of cristobalite (SiO₂) [27,28]. The silica structure (amorphous and/or crystalline) depends mainly on the husk’s calcination temperature. The ash produced by combustion at temperature range from 500 to 600 °C contains amorphous silica structure. The formation of cristobalite peak occurs at 700 °C and as the calcination temperature increases (above 800 °C), this peak becomes more intense [29,30]. The X-ray diffractogram obtained in the present study was similar to that reported by Cordeiro et al. [28] for combustion temperature at 950 °C. Under such conditions and using the refinement method for determining the amorphous index, Cordeiro et al. [29] verified that the ashes contain approximately 70% of amorphous silica in its composition.

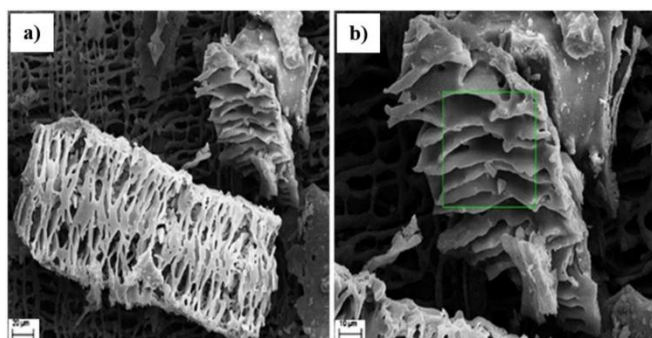


FIGURE 2. SEM IMAGES FOR RHA SAMPLES: (A) 1000X; (B) 2000X MAGNIFICATIONS.

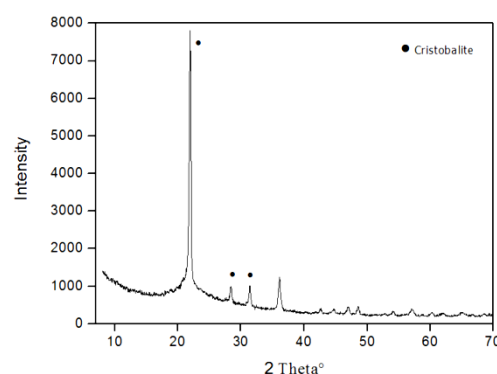


FIGURE 3. X-RAY DIFFRACTION OF THE ORIGINAL SAMPLE OF RICE HUSK ASH.

The chemical composition of the RHA summarized in Table 6 demonstrated the presence of inorganic components, mainly SiO₂ (≈ 90%) which is in agreement with data reported in the literature [31,32], revealing silica contents in the range from 90 to 95%, and the remainder consisting by other inorganic components.

TABLE 6
CHEMICAL COMPOSITION OF RICE HUSK ASH

Composition	SiO ₂	K ₂ O	CaO	P ₂ O ₅	MgO	MnO	Others	LOI
% mass	89.55	1.63	0.84	0.74	0.44	0.32	0.67	5.80

LOI: Loss on ignition.

The infrared spectrum of RHA displayed in Fig. 4 shows the positions and intensity of typical silica bands, the main constituent of the ashes. The bands at 1090 cm⁻¹ and 475 cm⁻¹ are assigned to the asymmetric and symmetric deformation of the Si-O-Si group, respectively. The band at 800 cm⁻¹ is assigned to the ring structure of the SiO₄ tetrahedron, and 3450 cm⁻¹

to the O-H stretch of the silanol groups present on the ash surface [24, 29,33]. As can be observed, the different samples, i.e. RHA *in natura* (RHA), RHA activated with methanol, and RHA contained adsorbed glycerol, presented different intensity of peaks relating to the silanol group.

Table 4 shows the areas of Si-OH peaks integration in order to relate them with the concentration of this compound in the studied samples. Both the RHA *in natura* and RHA activated with methanol show similar integration areas, demonstrating that there was no increase in the concentration of the Si-OH group on the surface of the ash. On the other hand, the RHA recovered after the glycerol removal, exhibited an integration area, which is 3.6 times greater than that of the RHA *in natura*. Furthermore, it was possible to observe the emergence of a small band at 2956 cm^{-1} that is assigned to the deformation of the C-H group. An increase in the area of the Si-OH group and the development of the C-H group can be related to a glycerol removal by the ash, demonstrating the efficiency of this sorbent in biodiesel purification processes.

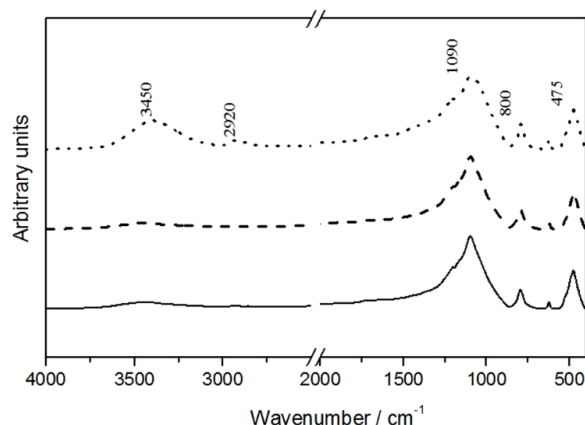


FIGURE 4. FTIR SPECTRA OF RICE HUSK ASH SAMPLES: SOLID LINE (RHA *IN NATURA*), DASH LINE (ACTIVATED RHA WITH METHANOL) AND DOT LINE (ACTIVATED RHA CONTAINING GLYCEROL ADSORBED).

TABLE 4
AREAS OF THE INTEGRATION PEAKS AT 3450 cm^{-1} FOR SAMPLES OF RICE HUSK ASH ANALYZED BY FT-IR.

Samples	Peak area at 3450 cm^{-1} (Si-OH)	Ratio $RHA_{mod.} / RHA_{in\ nat.}$
RHA (<i>in natura</i>)	58	-
RHA activated with methanol	60	1.0
Activated RHA containing glycerol adsorbed	211	3.6

IV. CONCLUSION

This study demonstrated the applicability of statistical designs to optimize the conditions that maximize the glycerol removal by dry washing. Under optimized conditions, the RHA showed promising results as a sorbent agent, providing high-quality biodiesel in accordance with the specifications established by ASTM D 6751 and EN 14214 standards. In addition, this sorbent showed similar performance to the conventional aqueous washing and adsorption with commercial resin, such as Amberlite. The adsorptive capacity of the RHA can be related to the high content of silica in its composition, as demonstrated by EDS, XDR and FT-IR analysis. RHA is a low-cost agricultural waste with high-availability features, hence being a promising material to be used in biodiesel purification processes.

ACKNOWLEDGEMENTS

The authors gratefully acknowledge the financial support of CNPq (Conselho Nacional de Desenvolvimento Científico e Tecnológico-Process Number 404812/2013-9). Leyvison Rafael V. da Conceição would especially like to thank the support of Coordenação de Aperfeiçoamento de Pessoal de Nível Superior (CAPES).

REFERENCES

- [1] Atadashi, I.M., Aroua, M.K., Aziz, A.A., 2011a. Biodiesel separation and purification: a review. *Renew. Energy* 36, 437-443.
- [2] Berrios, M., Skelton, S.L., 2008. Comparison of purification methods for biodiesel. *Chem. Eng. J.* 144, 459-465.
- [3] Lôbo, I.P., Ferreira, S.L.C., Cruz, R.S., 2009. Biodiesel: quality parameters and analytical methods. *Quim. Nova* 32, 1596-608.

- [4] Atadashi, I.M., Aroua, M.K., Aziz, A.R.A., Sulaiman, N.M.N., 2011b. Refining technologies for the purification of crude biodiesel. *Appl. Energy* 88, 4239–4251.
- [5] Veljković, V.B., Banković-ilić, I.B., Stamenković, O.S., 2015. Purification of crude biodiesel obtained by heterogeneously-catalyzed transesterification. *Renewable Sustainable Energy Rev.* 49, 500–516.
- [6] Rossetto, E., Beraldin, R., Penha, F.G., Pergher, S.B.C., 2009. Bentonites diatomites clays characterization and application in adsorption. *Quim. Nova* 32, 2064–2067.
- [7] Stojkovic, I.J., Stamenkovic, S.O., Povrenovic, D.S., Veljkovic, V.B., 2014. Purification technologies for crude biodiesel obtained by alkali-catalyzed transesterification. *Renewable Sustainable Energy Rev.* 32, 1–15.
- [8] Atadashi, I.M., 2015. Purification of crude biodiesel using dry washing and membrane technologies. *Alexandria Eng. J.* 54, 1265-1272.
- [9] Berrios, M., Martin, M.A., Chica, A.F., Martin, A., 2011. Purification of biodiesel from used cooking oils. *Appl. Energy* 88, 3625–3631.
- [10] Gomes, M.G., Santos, D.Q., Morais, L.C., Pasquini, D., 2015. Purification of biodiesel by dry washing, employing starch and cellulose as natural adsorbent. *Fuel* 155, 1–6.
- [11] Vasques, E.D.C., Granhen Tavares, C.R., Yamamoto, C.I., Mafra, M.R., Igarashi-Mafra, L., 2013. Adsorption of glycerol, monoglycerides and diglycerides present in biodiesel produced from soybean oil. *Environ. Technol.* 34, 2361–2369.
- [12] Na-Ranong, D., Leongpong, P. L., Khambung, S., 2015. Removal of steryl glucosides in palm oil based biodiesel using magnesium silicate and bleaching earth. *Fuel* 143, 229–235.
- [13] De Paula, A.J.A., Krugel, M., Miranda, J. O., Rossi, L.F.S., Neto, P.R.C., 2011. Utilização de argilas para purificação de biodiesel. *Quim. Nova* 34, 91–95.
- [14] Cernoch, M., Hajek, M., Skopal, F., 2010. Ethanolysis of rapeseed oil; distribution of ethyl esters, glycerides and glycerol between ester and glycerol phases. *Bioresour. Technol.* 101, 2071–2075.
- [15] Dias, J.M., Santos, E., Santos, F., Carvalho, F., Alvin-Ferraz, M.C.M., Almeida, M.F., 2014. Study of an ethylic biodiesel integrated process: Raw-materials, reaction optimization and purification methods. *Fuel Process. Technol.* 124, 198–205.
- [16] Amberlyst: Users Guide. Available at http://www.ags.rs/dow/pdf/biodiesel_bd10dry_userguide_sep08.pdf. Accessed in 26 October 2016.
- [17] Carvalho, A.K.F., 2011. Síntese de biodiesel por transesterificação pela rota etílica: comparação do desempenho de catalisadores heterogêneos. 105p. MSc Dissertation - Escola de Engenharia de Lorena, Universidade de São Paulo, Lorena (2011). Available at <http://www.eel.usp.br>
- [18] Bondioli, P., Bella, L.D., 2005. An alternative spectrophotometric method for the determination of free glycerol in biodiesel. *Eur. J. Lipid Sci. Technol.* 107, 153–157.
- [19] Paiva, E.J.M., da Silva, M.L.C.P., Barboza, J.C.S., Oliveira, P.C., de Castro, H.F., Giordani, D. S., 2013. Non-edible babassu oil as a new source for energy production - a feasibility transesterification survey assisted by ultrasound, *Ultrason Sonochem.* 20, 833–838.
- [20] Andrade, G.S.S., Carvalho, A.K.F., Romero, G.M., Oliveira, P.C., De Castro, H.F., 2014. *Mucor circinelloides* whole-cells as a biocatalyst for the production of ethyl esters based on babassu oil. *Bioprocess Biosyst. Eng.* 37, 2539–2548.
- [21] Nelder, J.A., 1998. The selection of terms in response surface models-how strong is the weak heredity principle? *The American Statistical* 52, 315–318.
- [22] Ruthven, D.M., 1984. Principles of adsorption and adsorption process. United States of America: Wiley – Interscience Publication 1–13, 221–270.
- [23] Rêgo, J.H.S., Nepomuceno, A.A., Figueiredo, E.P., Hasparyk, N.P., 2015. Microstructure of cement pastes with residual rice husk ash of low amorphous silica content. *Constr. Build. Mater* 80, 56–68.
- [24] Manique, M.C., Faccini, C.S., Onorevoli, B., Benvenuti, E.V., Caramão, E.B., 2012. Rice husk ash as an adsorbent for purifying biodiesel from waste frying oil. *Fuel* 92, 56–61.
- [25] Foletto, E.L., Hoffmann, R., Hoffmann, R.S., Portugal Júnior, U.L., Jahn, S.L., 2005. Aplicabilidade das cinzas da casca de arroz. *Quim. Nova* 28, 1055–1060.
- [26] Kim, M., Yoon, S.H., Choi, E., Gil, B., 2008. Comparison of the adsorbent performance between rice hull ash and rice hull silica gel according to their structural differences. *LWT Food Science and Technol.* 41, 701–706.
- [27] Antiohos, V.G., Papadakis, V.G., Tsimas, S., 2014. Rice husk ash (RHA) effectiveness in cement and concrete as a function of reactive silica and fineness. *Cem. Concr. Res.* 61–62, 20–27.
- [28] Cordeiro, G.C., Filho, R.D.T., Tavares, L.M., Fairbairn, E.M.R., Hempel, S., 2011. Influence of particle size and specific surface area on the pozzolanic activity of residual rice husk ash. *Cem. Concr. Compos* 33, 529–534.
- [29] Cordeiro, L.N.P., Masuero, A.B., Dal Molin, D.C.C., 2014. Análise do potencial pozolânico da cinza de casca de arroz (CCA) através da técnica de refinamento de Rietveld. *Revista Mat.* 19, 150–158.
- [30] Bie, R.S., Song, X.F., Liu, Q.Q., Ji, X.Y., Chen, P., 2015. Studies on effects of burning conditions and rice husk ash (RHA) blending amount on the mechanical behavior of cement. *Cem. Concr. Compos* 55, 162–168.
- [31] Le, H.T., Ludwig, H.M., 2016. Effect of rice husk ash and other mineral admixtures on properties of self-compacting high performance concrete. *Mater. Des.* 89, 156–166.
- [32] Hwang, C.J., Huynh, T.P., 2015. Effect of alkali-activator and rice husk ash content on strength development of fly ash and residual rice husk ash-based geopolymers. *Constr. Build. Mater* 101, 1–9.
- [33] Vlaev, L., Petkov, P., Dimitrov, A., Genieva, S., 2011. Cleanup of water polluted with crude oil or diesel fuel using rice husk ash. *J. Taiwan Inst. Chem. Eng.* 42, 957–964.